



ELSEVIER

Surface Science 382 (1997) L705–L712

surface science

Surface Science Letters

Silicide growth at metal surfaces: competition between subsurface diffusion and chemical reaction

Nicolas Wälchli, Elisabeth Kampshoff *, Alexander Menck, Klaus Kern

Institut de Physique Expérimentale, EPFL, CH-1015 Lausanne, Switzerland

Received 26 April 1996; accepted for publication 25 February 1997

Abstract

The nucleation and growth of silicide monolayers during deposition of Si on Pd(110) has been studied in situ by scanning tunnelling microscopy and vibrational spectroscopy of adsorbed CO. The growth scenario is found to depend strongly on the deposition temperature, which determines the competition between Si subsurface diffusion and silicide formation. With increasing temperature amorphous silicon (< 140 K), amorphous silicide (140–320 K) and crystalline palladium silicide (> 320 K) grows at the metal surface. Below 450 K the ordered silicide grows in strained islands while above 450 K strain is partially relieved through misfit dislocations. © 1997 Elsevier Science B.V.

Keywords: Growth; Infrared absorption spectroscopy; Metal-semiconductor interfaces; Palladium; Scanning tunneling microscopy; Silicon

Silicide formation at metal–silicon interfaces has been studied extensively, both because of its practical importance in semiconductor technology and because epitaxial silicide films provide well-defined model systems for basic studies of interface reactions [1–5]. Much has been learned of these fascinating systems, however, a complete microscopic understanding of the mechanisms for silicide formation at the interface is still lacking. Moreover, nearly all experimental studies of silicide formation concerned the reaction of deposited metals on silicon surfaces; the inverse scenario – Si deposition on metal surfaces – has rarely been studied [6].

In this Letter we report in situ scanning tunnelling microscopy (STM) and reflection absorption infrared spectroscopy (RAIRS) results on silicide

formation during Si deposition on the Pd(110) surface. The crucial parameter for the silicide growth is the deposition temperature, which determines the competition between Si subsurface diffusion and silicide formation. Despite the immiscibility of Pd and Si in the bulk, silicon is found to dissolve in the selvage of the Pd crystal. The present system thus constitutes a further example of surface mixing of elements immiscible in the bulk; a phenomenon which was predicted many years ago [7] but uncovered experimentally only recently for metal-on-metal [8,9] and metal-on-semiconductor systems [10,11]. Below 140 K Si does not react with the Pd surface and amorphous silicon clusters form during deposition. With increasing temperature Si penetrates into the metal surface and silicide is formed. Between 140 and 320 K the silicide is amorphous, while above 320 K

* Corresponding author. Fax: +44 21 6933604.

it is crystalline growing in well shaped islands. The silicide islands are found to be unstable at elevated temperatures.

The experiments were carried out in an UHV chamber (base pressure 2×10^{-10} mbar) equipped with standard surface analysis facilities, a variable temperature STM (150–600 K) and a FTIR spectrometer (Mattson GALAXY 6020) [12]. The Pd(110) crystal was prepared by cycles of 800 eV Ar⁺ ion sputtering at 300 and 700 K, heating at 600 K in a 10^{-6} mbar O₂ atmosphere and flash annealing at 900 K. The surface quality was controlled by STM, LEED and AES. STM images reveal large terraces with an average size of ~ 500 – 1000 Å. Evaporation of Si on the well prepared Pd(110) surface was achieved by electron bombardment heating of a Si rod. The calibration of the deposition rate was done by means of STM and RAIR spectroscopy of adsorbed CO at $T = 100$ K. At low coverages the Si growth is found to be two-dimensional and the area covered by Si and the IR signal of Si bound CO is a direct measure for the Si dosage assuming a sticking coefficient of one. Typical deposition rates were of the order of 5×10^{-4} ML s⁻¹. All STM measurements were performed in the constant current mode at 0.5–2 V bias and 0.5–1.5 nA tunnelling current. The adsorption of CO on the Si/Pd(110) surfaces was investigated by RAIRS. All spectra were taken in reflection geometry and with a resolution of 8 cm⁻¹. The CO was dosed onto the surface at 100 K; monolayer coverage was achieved after exposure of 40 L.

The combination of STM and RAIRS offers a unique possibility of correlating surface chemical analysis with atomic-level surface structure. This is particularly important in the case of very reactive systems like Si/Pd. As chemical sensor we use the CO molecule which is adsorbed onto the well-prepared and characterised heterogeneous surfaces. The internal stretch vibration which is easily accessible with RAIRS reacts quite sensitively to the chemical nature of its surrounding and it is thus a valuable probe of the surface chemical composition.

At low temperatures (< 140 K) Si does not react with the Pd(110) surface. The Auger spectrum

shows only one single peak at 92 eV demonstrating the absence of silicide formation [11]. The unreactive deposition at low temperatures is confirmed by vibrational spectroscopy of adsorbed CO. Fig. 1a shows as reference the infrared absorption of CO adsorbed on amorphous Si (a-Si). A single band is revealed at 2104 cm⁻¹ with a linewidth of 19 cm⁻¹. Upon deposition of Si onto the clean Pd(110) surface at a temperature below 140 K the same vibrational band is detected (Fig. 1b). There is no significant shift visible indicating the absence of any reaction with the Pd substrate. The second absorption band around 2000 cm⁻¹ is easily determined as being due to CO adsorbed on the remaining, uncovered Pd substrate sites (compare with Fig. 1c) characterising CO adsorption on clean Pd(110) in bridge configuration. Both vibrational bands of the Si/Pd(110) surface are inhomogeneously broadened indicating that the clusters of

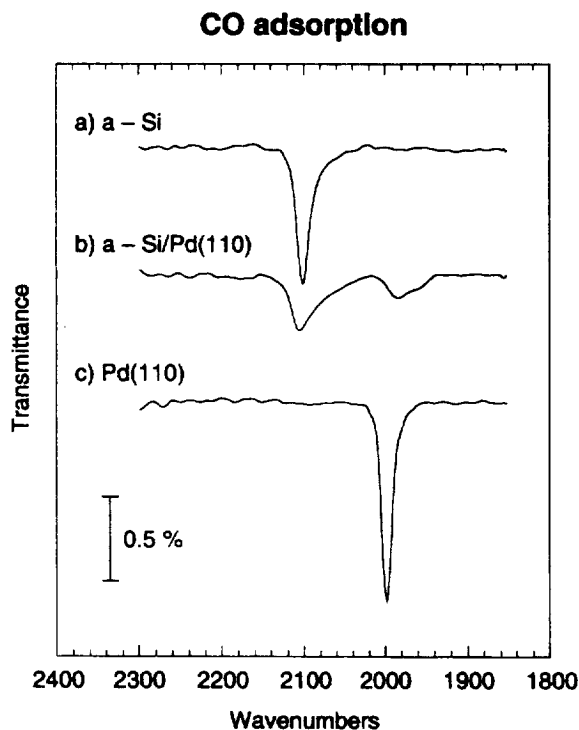


Fig. 1. The infrared spectra of a monolayer of CO adsorbed on amorphous Si (a), on Si/Pd(110) after deposition of 1.2 ML Si at 100 K (b) and on clean Pd(110) (c). A monolayer was achieved after dosing 40 L CO at 100 K.

amorphous Si and the remaining patches of Pd substrate are small and randomly distributed.

Above 140 K the deposition of Si on Pd(110) is reactive. Auger spectroscopy shows multiple peak shape features around 92 eV characteristic for palladium-silicide formation [11]. The silicide formation is also evident in the vibrational spectra of chemisorbed CO. Three representative spectra of CO adsorbed on silicide/Pd(110) are shown in Fig. 2. One monolayer CO was dosed onto the surfaces at 100 K after Si deposition at 300 K (a), 400 K (b) and 550 K (c). The three IR spectra are similar. They show two distinct absorption bands: a low frequency band at 2000 cm^{-1} and a high frequency band at 2074 cm^{-1} (b, c) and 2090 cm^{-1} (a), respectively. The low frequency mode corresponds to CO bound in bridge position to Pd atoms of the uppermost layer, while the high frequency mode indicates the presence of Si in this

layer. The silicide formation is evident by comparing the spectra with the analogous spectrum of amorphous Si on Pd(110) in Fig. 1b. The frequency has red-shifted by 30 cm^{-1} upon Si deposition at and above 400 K and by 14 cm^{-1} upon deposition at room temperature. As will become clear below by comparing the IR data to the STM measurements, the band at 2074 cm^{-1} is characteristic for crystalline silicide while the broad vibrational band at 2090 cm^{-1} corresponds to CO adsorption on small amorphous silicide clusters.

The growth morphology has been studied in the same temperature range (100–600 K) by variable temperature STM. At low temperatures ($<140\text{ K}$) a high density of very small Si clusters nucleates on the Pd(110) surface (not shown here). Upon increasing the temperature above 140 K amorphous silicide clusters are formed. Fig. 3 shows as an example the nucleation of palladium silicide clusters at 300 K after deposition of 0.06 ML Si. The clusters formed at room temperature have a

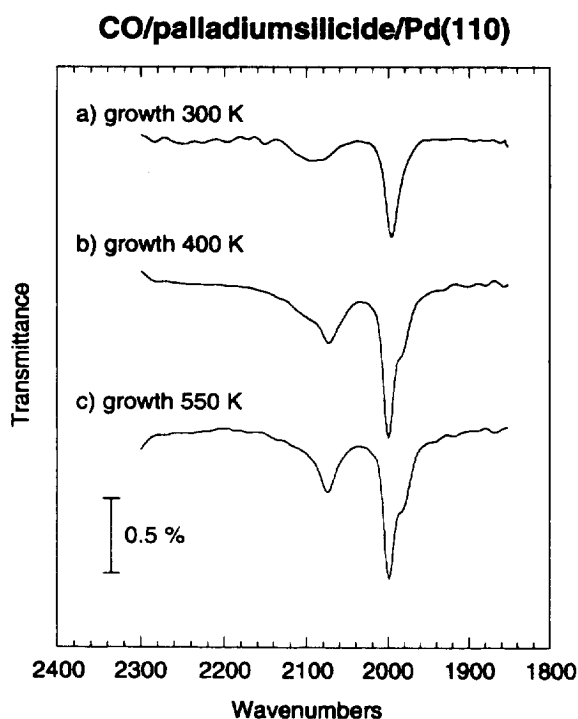


Fig. 2. The infrared spectra of a monolayer of CO adsorbed on the palladium-silicide/Pd(110) surface after deposition of 0.9 ML Si at 300 K (a), 1.2 ML Si at 400 K (b) and 1.2 ML Si at 550 K (c). A monolayer was achieved after dosing 40 L CO at 100 K.



Fig. 3. The growth of amorphous palladium silicide clusters on Pd(110) at 300 K; Si deposition ~ 0.06 ML. Characters mark silicide clusters (SC), substrate holes (SH) and Pd adatom clusters (AC).

typical size of 10–40 Å and are uniformly distributed at the surface. The corresponding LEED pattern is diffuse indicating that the clusters have no crystalline structure but are amorphous. Comparing this surface morphology with the infrared spectra of Fig. 2a the anomalously large linewidth becomes quite reasonable. It is likely to be a consequence of both, the small size of the silicide clusters and their amorphous structure. The silicide formation on Pd(110) bears analogies to the initial growth of palladium-silicide on Si(111) at room temperature where also the formation of amorphous silicide clusters has been observed [13].

The STM image in Fig. 3 reveals a very interesting feature concerning the silicide formation at room temperature: besides the silicide reaction also a noticeable subsurface diffusion of deposited Si takes place. This is evident in the surface morphology which shows besides the silicide clusters (SC) the presence of two additional surface structures: substrate holes (SH) and Pd adatom islands (AC). The substrate holes are mostly one monolayer deep and are elongated along the $[\bar{1}10]$ direction; they are mono- or diatomic in width. In addition to these holes we find a small number of adatom islands (AC), which are arranged as short chains also running along $[\bar{1}10]$. From our homoepitaxy experiments on the Pd(110) surface we know that Pd atoms deposited at room temperature nucleate in the form of dimer chains running along the easy $[\bar{1}10]$ direction [14]. We can thus identify the chain like clusters (AC) as Pd adatom islands.

A likely scenario to explain this morphology is the following. Upon deposition some Si adatoms penetrate into the substrate by exchanging their place with Pd atoms of the top surface layer. Since we observe holes in the substrate (SH) it is likely to assume that some of the incorporated Si atoms leave the surface sites and diffuse deeper into the Pd bulk. This process might be explained as follows. A nearby Pd atom in the surface layer is ejected to create a vacancy, which then can be filled by a Pd atom from the second layer exchanging its place with the Si atom in the first layer. The kicked out Pd atoms can diffuse and form Pd adatom islands (AC); the Pd adatoms in addition can react with Si adatoms to form silicide clusters

(SC). Due to the anisotropic structure of the substrate, vacancy-islands and Pd-adislands are elongated along $[\bar{1}10]$ at room temperature [14]. This mechanism ensures an efficient subsurface diffusion of Si and is compatible with the morphology seen in Fig. 3. It is interesting to note that a very similar scenario as reported above for Si subsurface diffusion has been observed in the case of Au mixing into Ni(110) [8] and H penetration into the (110) surfaces of Pd [15] and Ni [16]. Also, in these cases the substrate penetration seems to occur via coupled exchange processes generating substrate holes and adislands.

Above about 320 K the reaction scenario is different. As an example we show in Fig. 4 two STM images characterising the silicide formation at 400 K after deposition of 0.4 and 0.6 ML Si. Two kinds of well shaped silicide islands are formed: one embedded in the first Pd layer and the other on the Pd(110) surface, one step height above. Both island types are rhomboid. There are two domains visible which are oriented along the diagonal $[\bar{1}12]$ and $[\bar{1}\bar{1}2]$ directions of the Pd(110) surface unit cell. The adislands and the embedded islands show the same distinct orientations. The silicide islands have a crystalline structure and grow epitaxially on the Pd(110) substrate indicated by a sharp $\left(\frac{1}{4} \frac{1}{2}\right)$ LEED superstructure with two domains. A detailed analysis of the LEED and FTIR measurements reveals a Pd₂Si stoichiometry of the silicide islands [17].

Obviously the embedded silicide islands are formed by the direct reaction of Pd in the surface layer with impinging Si atoms, while the adislands are formed through reaction of ejected Pd adatoms with Si adatoms. The density of the embedded silicide islands is much higher than that of the adislands. This can be understood because the flux of Si atoms arriving at the Pd surface is larger than the “effective flux” of Pd adatoms ejected onto the surface due to the Si–Pd exchange. The nucleation probability of embedded silicide islands is thus higher than the probability that Si and Pd adatoms meet and nucleate an adisland.

With further increasing temperature migration becomes increasingly faster with respect to deposition, i.e. the nucleation density decreases and only

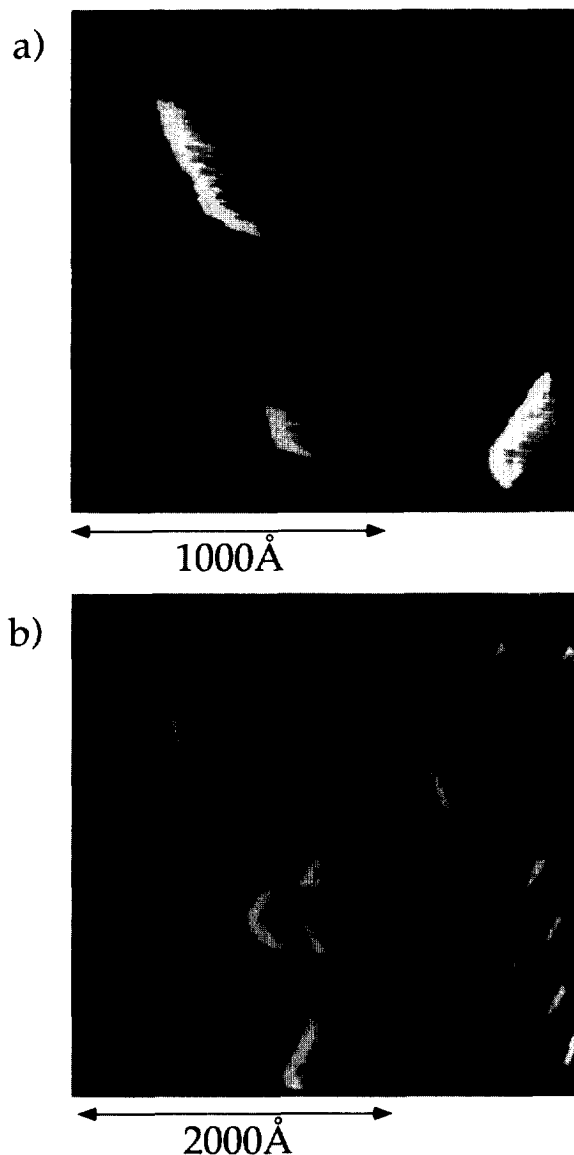


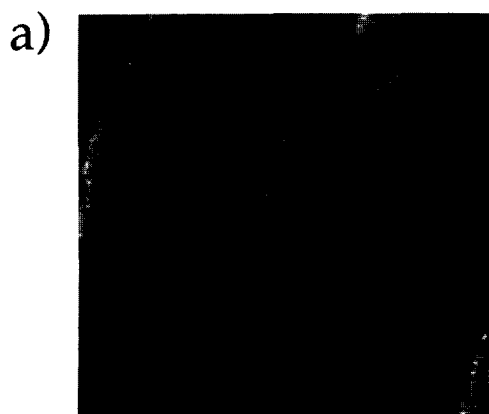
Fig. 4. The growth of crystalline palladium silicide islands on Pd(110) at 400 K. The Si dosage at the surface is 0.4 ML (a) and 0.6 ML (b); the STM images have been taken immediately after deposition.

few very large embedded silicide islands grow (Fig. 5). A pattern of parallel dark stripes visible on the silicide islands attracts particular attention. The depression stripes running along the $[\bar{1}12]$ direction are ~ 9 Å in width and have an average separation of ~ 45 Å. We identify these stripes as

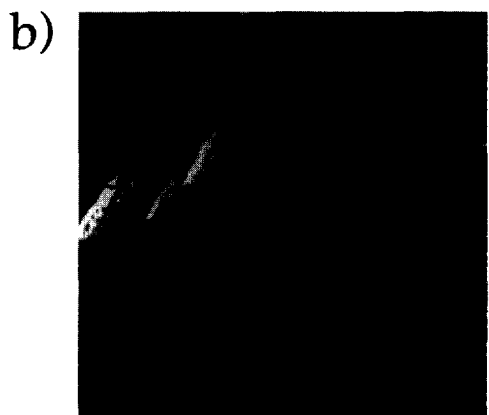
misfit dislocations partially relieving the strain [18]. The silicide must thus be under substantial compressive strain and islands can only grow coherent up to a critical size. Larger islands have to relieve their strain by the introduction of misfit dislocations. The LEED measurements reveal the same $\begin{pmatrix} 1 & 1 \\ 4 & 0 \end{pmatrix}$ pattern with additional spot splittings along the diagonals; indicating that the silicide in between the misfit dislocations has the same crystalline structure as the coherent islands grown at 400 K.

It is quite interesting to compare Fig. 4a with Fig. 5a. In both cases the STM images were taken directly after 0.4 ML Si deposition at 400 and 550 K, respectively. Obviously the amount of silicide, which is formed at the substrate surface, is different. The surface area, which is covered with silicide in Fig. 5a, is about twice as large as the one shown in Fig. 4a. In general we observe a pronounced formation of surface silicide at 550 K indicating an increase in silicide reaction at the surface in disfavour of subsurface diffusion with increasing temperature. Taking account of the stoichiometry of Pd_2Si we can estimate that at 550 K more than half of the deposited Si is buried below the surface directly after deposition. At 400 K the fraction of subsurface Si is of the order of 75%.

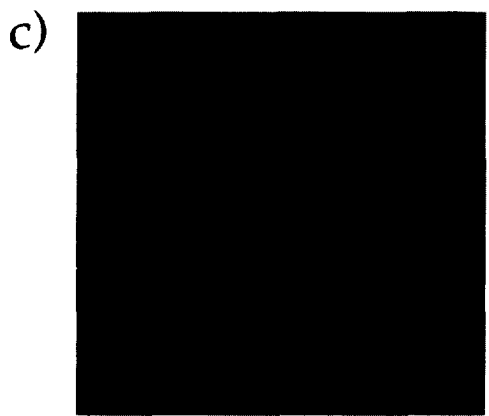
It is important to note that the crystalline silicide is not stable at elevated temperatures. At ~ 500 K the islands dissolve on a minute time scale while at temperatures ~ 400 K typical decay times are of the order of hours. This is demonstrated in Fig. 5c imaging the Pd(110) surface 60 min after Si deposition at 550 K (the temperature was kept at 550 K). The entire silicide islands have decomposed (compare with Fig. 5a showing the same surface immediately after deposition), and the Si has disappeared leaving a flat Pd surface with some small holes. As already seen in Fig. 3 these holes are characteristic for the subsurface diffusion of Si via an exchange process with the Pd substrate atoms. It is most likely to assume that the Si atoms, which are released during the silicide decomposition, diffuse subsurface and bury below the surface. Coarsening of the crystalline silicide into 3D clusters at the surface can be excluded.



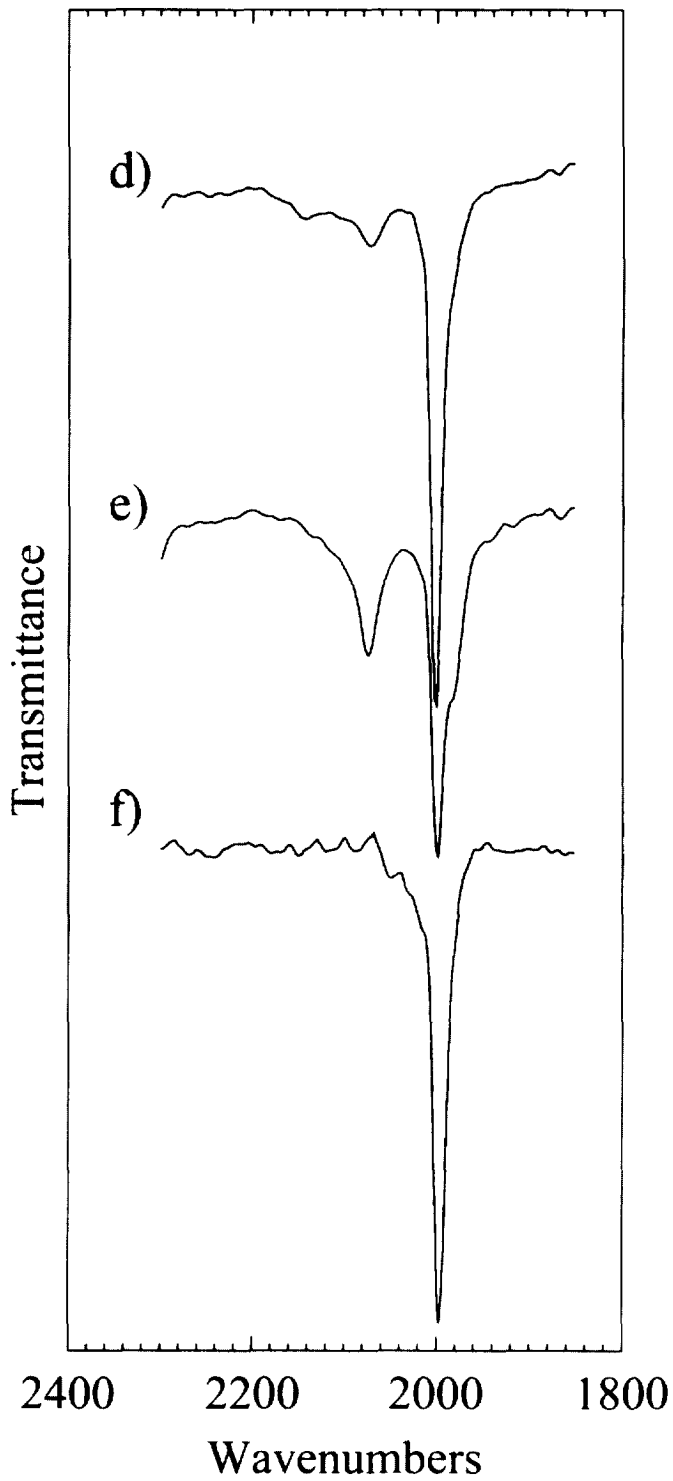
400 Å



400 Å



400 Å



The large scale image in Fig. 5c shows no hints of 3D clusters on the flat terrace as well as at step edges. We have scanned many different zones always observing similar flat Pd terraces with small holes.

The RAIR-spectra on the right-hand side of Fig. 5 give additional evidence that the dissolution of the silicide is not a local effect associated with the limited image field of the STM. The infrared experiment is an integral probe sampling the entire macroscopic surface. It is clearly seen that the vibrational band at 2074 cm^{-1} (characteristic for the presence of Si at the surface) has disappeared completely after keeping the surface at 550 K for 60 min, while the Pd-peak at 2000 cm^{-1} has gained intensity (Fig. 5f). Thus, the vibrational spectra demonstrate that the entire surface is completely Pd terminated and that Si has diffused subsurface. It is, however, important to note that the Si dissolving into the substrate does not “disappear” completely into the bulk. This behaviour is revealed by Auger spectroscopy showing that the Si AES peak decreases but does not disappear completely within several hours indicating the presence of the silicon in the selvage just beneath the surface.

The observed growth scenario can be understood qualitatively in the following picture. Si deposited on the Pd surface has two reaction channels leading to the global and the local energy minimum of the system, respectively. The local minimum is achieved via silicide reaction at the surface, but this state is found to be unstable at elevated temperatures. After decomposition of the entire silicide islands a flat, Pd terminated surface is left. Thus, the energetic ground state of the system is the mixing of Si in the selvage of the Pd substrate. This state is achieved through subsurface diffusion of the Si atoms via a Si–Pd exchange mechanism. As both processes, chemical reaction and subsurface diffusion are thermally activated

processes, the corresponding reaction rates depend exponentially on their activation barriers. At very low temperatures both reaction channels are frozen and unreacted Si nucleates at the surface. With increasing temperature the reaction channel with the lowest energy barrier becomes first populated. Reaching a certain temperature also the higher energy barrier can be overcome and the population into the second channel will be observed. Since the nucleation of the silicide islands is only possible by Si atoms penetrating the substrate it is natural to assume that the barrier for interdiffusion is lower than the chemical activation energy for silicide formation. The pronounced formation of surface silicide at elevated temperatures confirms this assumption. Thus with increasing temperature first subsurface diffusion becomes active. Only at elevated temperatures does silicide formation becomes significant; first amorphous then crystalline silicide is formed.

From the early work of Okada et al. [11] it is already known that the volume phase diagram of Si/Pd fails in describing processes which proceed at the surface. In case of Pd deposited on the Si substrate the deposit penetrates the surface although there is no miscibility indicated in the phase diagram. Later work from Nishigaki et al. confirmed these results [19]. Silicon on Pd(110) constitutes a further example for the surface mixing of elements, which are immiscible in the bulk. Recent theoretical analysis suggests that surface mixing is expected generally in systems which are dominated by atomic size mismatch [20,21]. While the mismatch renders the elements immiscible in the bulk, the reduced strain energy at the surface will cause a finite miscibility there. An interesting difference between the present system and the previously studied systems [7–10] is the fact that for Si/Pd(110) the intermixing is not confined to the topmost surface layer but rather to the first few layers just beneath the surface.

Fig. 5. Left-hand side: the growth (a, b) and dissolution (c) of crystalline palladium silicide on Pd(110) at 550 K. The amount of Si deposited is 0.4 ML (a) and 1.2 ML (b); the STM images have been taken immediately after deposition. The STM image in (c) shows the surface (a) 60 min after deposition while keeping the temperature at 550 K. Right-hand side: the corresponding infrared spectra of a monolayer of CO adsorbed on the palladium-silicide/Pd(110) surface; deposition of 0.8 ML (d) and 1.2 ML (e) Si at 550 K. The spectrum in (f) corresponds to situation (c) where the surface was kept at 550 K after silicon deposition.

References

- [1] V.G. Lifshits, A.A. Saranin, A.V. Zotov, *Surface Phases on Silicon: Preparation, Structures, and Properties*, Wiley, New York, 1994.
- [2] K.N. Tu, J.W. Mayer, in: *Thin Films – Interdiffusion and Reaction*, Wiley, New York, 1978.
- [3] P.A. Bennet, B. DeVries, I.K. Robinson, P.J. Eng, *Phys. Rev. Lett.* 69 (1992) 2539.
- [4] S.P. Muraka, *Silicides for VLSI Applications*, Academic, New York, 1983.
- [5] X. Tong, J.M. Gibson, *Appl. Phys. Lett.* 65 (1994) 168.
- [6] M.C. Munoz, F. Soria, J.L. Sacedon, *Surf. Sci.* 189/190 (1987) 204;
A. Franciosi, D.W. Nilas, G. Margaritondo, C. Quaresima, M. Capozzi, P. Perfetti, *Phys. Rev. B* 32 (1985) 6917;
M.A. Chester, A.B. Horn, *J. Phys.: Condens. Matter* 3 (1991) 251;
K. Nishimori, H. Tokutaka, H. Sumi, N. Ishihara, *J. Vac. Soc. Japan* 34 (1991) 143.
- [7] B. Mutaftschiev, A. Bonnissent, *Surf. Sci.* 34 (1973) 649.
- [8] L.P. Nielsen, *Phys. Rev. Lett.* 71 (1993) 754.
- [9] H. Röder, R. Schuster, H. Brune, K. Kern, *Phys. Rev. Lett.* 71 (1993) 2086.
- [10] R.M. Tromp, A.W. Denier van der Gon, M.C. Reuter, *Phys. Rev. Lett.* 68 (1992) 2313.
- [11] S. Okada, K. Oura, T. Hanawa, K. Satoh, *Surf. Sci.* 97 (1980) 88.
- [12] E. Hahn, A. Fricke, H. Röder, K. Kern, *Surf. Sci.* 297 (1993) 19.
- [13] U.K. Köhler, J.E. Demuth, R.J. Hamers, *Phys. Rev. Lett.* 60 (1988) 2499;
L. Casalis, C. Casati, R. Rosei, M. Kiskinova, *Surf. Sci.* 331–333 (1995) 381.
- [14] E. Kampshoff, N. Waelchli, K. Kern, to be published; See also J.P. Bucher, E. Hahn, P. Fernandez, C. Massobrio, K. Kern, *Europhys. Lett.* 27 (1994) 473.
- [15] E. Kampshoff, N. Waelchli, A. Menck, K. Kern, *Surf. Sci.* 360 (1996) 55.
- [16] L.P. Nielsen, F. Besenbacher, E. Laegsgaard, I. Stensgaard, *Phys. Rev. B* 44 (1991) 13156.
- [17] E. Kampshoff, N. Waelchli, A. Menck, K. Kern, to be published.
- [18] H. Brune, H. Röder, C. Boragno, K. Kern, *Phys. Rev. B* 49 (1994) 2997.
- [19] S. Nishigaki, T. Komatsu, M. Arimoto, M. Sugihara, *Surf. Sci.* 167 (1986) 27.
- [20] J. Tersoff, *Phys. Rev. Lett.* 74 (1995) 434.
- [21] M. Schmid, *Phys. Rev. B* 51 (1995) 10937.